Like a Rolling Stone: Effects of Space Deformation During Linear Acceleration on Slope Perception and Cybersickness

Tongyu Nie* Isayas Berhe Adhanom Evan Suma Rosenberg

University of Minnesota

Figure 1: A virtual environment (a) with proposed geometry transformations. When users accelerate or decelerate, the VE will be transformed into an uphill (b) or downhill (c) slope.

Abstract

The decoupled relationship between the optical and inertial information in virtual reality is commonly acknowledged as a major factor contributing to cybersickness. Based on laws of physics, we noticed that a slope naturally affords acceleration, and the gravito-inertial force we experience when we are accelerating freely on a slope has the same relative direction and approximately the same magnitude as the gravity we experience when standing on the ground. This provides the opportunity to simulate a slope by manipulating the orientation of virtual objects accordingly with the accelerating optical flow. In this paper, we present a novel space deformation technique that deforms the virtual environment to replicate the structure of a slope when the user accelerates virtually. As a result, we can restore the physical relationship between the optical and inertial information available to the user. However, the changes to the geometry of the virtual environment during space deformation remain perceptible to users. Consequently, we created two different transition effects, pinch and tilt, which provide different visual experiences of ground bending. A human subject study (N=87) was conducted to evaluate the effects of space deformation on both slope perception and cybersickness. The results confirmed that the proposed technique created a strong feeling of traveling on a slope, but no significant differences were found on measures of discomfort and cybersickness.

Index Terms: Human-centered computing—Human computer interaction (HCI)—Interaction paradigms—Virtual reality; Computing methodologies—Computer graphics—Graphics systems and interfaces—Virtual reality;

1 Introduction

Continuous virtual locomotion is a common method for moving through a virtual environment (VE) without being constrained by the physical space like real walking or increasing users' spatial disorientation like teleportation or snap turning, but it can potentially cause severe cybersickness [8, 46, 68]. Cybersickness raises significant accessibility concerns as it discourages people from using VR, and prior research has also shown that it disproportionately affects women [48]. Consequently, research into both the causes of and potential mitigation techniques for cybersickness has become increasingly important as the usage of virtual reality technologies continues to expand across a variety of application domains.

In VR, users' virtual motions that can be inferred from artificial optical information that is decoupled from their physical movements relative to the Earth. Physical movements can change the gravito-inertial force (GIF) vector and stimulate the vestibular system. When standing still on a flat surface, the GIF is always equal to gravity and cannot be changed effectively by current technologies like optical information. Such discrepancies can result from technical issues, such as system latency, or caused by the choice of locomotion interface, such as controller-based continuous virtual locomotion. The decoupled relationship between the optical and inertial information in a simulated environment like VR is commonly acknowledged as a major factor contributing to cybersickness. Several different methods for mitigating cybersickness have been proposed, such as dynamic field-of-view (FOV) modification [7, 19] and static or dynamic rest frames [9]. However, these methods modify display characteristics in the user's visual field, often reducing the visibility of the virtual environment, which could have a potentially negative effect on the user's subjective experience [12, 55, 76].

In this paper, we introduce a geometry transformation to simulate a slope while accelerating in the VE. It is reasonable to assume that our perceptual systems are highly adapted to the physical laws in our environment [5]. By deforming the meshes in the VE, we can restore the physical relationship between the optical flow and the gravito-inertial force we perceive. However, space deformation modifies the geometry of the VE and could therefore introduce undesired effects for users. In general, the effectiveness and potential trade-offs of space deformation techniques have not yet been thoroughly investigated. To this end, we conducted a between-subjects user study with 87 participants to better understand the effects of space deformation on both **slope perception** and **cybersickness**. The results indicate that space deformation successfully induced strong feelings of being on a slope. However, no significant difference was found between the experimental and control groups on measures of discomfort and cybersickness. This suggests that the proposed space deformation technique may be well-suited for providing a subjective experience of walking on a slope, but further design iteration and evaluation are necessary to understand its impact on user comfort.

*e-mail: {nie00035, adhanom, suma}@umn.edu

2023 IEEE Conference Virtual Reality and 3D User Interfaces (VR) | 979-8-3503-4815-6/23/$31.00 ©2023 IEEE | DOI: 10.1109/VR55154.2023.00081

2642-5254/23/$31.00 ©2023 IEEE
DOI 10.1109/VR55154.2023.00081

2 Related Work

2.1 Cybersickness: Causes and Measures

Causes Cybersickness is a form of discomfort induced by VR experiences. Some of its symptoms are similar to those produced by motion sickness, while others, like oculomotor discomfort, are unique to cybersickness. Despite the existence of a few widely known hypotheses, there are still many knowledge gaps concerning causes of cybersickness and no universally accepted theory [65]. Sensory conflict theory has been regarded as a leading explanation for motion sickness by the research community, particularly VR experts, for decades [1, 29, 50, 58, 64]. Sensory conflict theory assumes that different sensory organs can specify motion independently, and we expect different organs to have expected patterns of input signals given particular voluntary commands [32, 34, 53]. Based on this assumption, sensory conflict claims that motion sickness is caused by a mismatch between current multi-sensory input/output patterns about self-motion and expected sensory input/output patterns based on previous experiences [32, 52]. Oman mathematically formulated this theory where the difference between expected and real sensor output is used to correct our mental model from an external disturbance in a way similar to the update phase of a Kalman Filter [52].

The postural instability theory is another theory to explain the causes of cybersickness [61]. This theory states that the cause of motion sickness is destabilization in control of the body. Overall body posture is strongly influenced by optical stimulation [35]. And in VR, there are optically specified accelerations and rotations that are unrelated to constraints on the control of the body because it is not accelerating [25]. As a result, our postural control strategies that are linked to optical information are inappropriate, which causes postural instability [61].

Measures The simulator sickness questionnaire (SSQ) is a comprehensive questionnaire that was designed to assess negative symptoms during the use of flight simulators and has become the most widely used instrument for measuring cybersickness before and after exposure to virtual reality [30]. The Fast Motion Sickness Score is a fast and simple method for monitoring participants' severity of sickness at a higher frequency; participants only need to report their feeling of motion sickness in a single question on a 20-point scale [31]. Fernandes and Feiner adapted the discomfort score from Rebenitsch and Owen, where participants were asked to rate their discomfort level on a scale of 0-10, with 0 being how they felt coming in, and 10 indicating that they want to stop [19, 59]. Dennison et al. explored the use of physiological signals to predict cybersickness [15]. The most relevant signals include electrocardiogram (ECG), electrogastrogram (EGG), electroencephalogram (EEG), and heart rate. The postural instability theory also suggests that spontaneous postural sway can be used to identify individuals who are more susceptible to cybersickness [6, 54, 62, 67]. The effectiveness of this approach was questioned by some researchers in different experimental settings [14, 38, 75]. However, Islam et al. found that head tracking data can be used to predict cybersickness together with other physiological data using machine learning [28].

2.2 Cybersickness Mitigation

Various methods have been previously proposed to mitigate cybersickness during continual virtual locomotion. Most of the software-based techniques, such as dynamic FOV restriction and peripheral blurring, are intended to reduce optical flow associated with visually-induced motion sickness. On the other hand, haptic techniques focus more on providing vestibular stimulus to mitigate sensory conflict.

Dynamic FOV Restriction Dynamic FOV restriction is one of the most widely used cybersickness mitigation techniques. This technique blocks the peripheral optical flow to reduce the available optical information [7]. Fernandes and Feiner have found that dynamic FOV restriction can mitigate cybersickness [19]. Further studies have shown its effectiveness on both sexes [1, 3]. Researchers have also proposed asymmetric variants of FOV restriction strategies for different types of locomotion tasks and virtual environments [2, 77–80]. Zhao et al. found that dynamically reducing peripheral image contrast was similarly effective as the black FOV restrictor [82]. However, FOV restriction is not always beneficial, and reducing the visibility of the virtual environment can potentially have a negative impact on the user experience [47, 51].

Peripheral Blurring Like FOV restriction, peripheral blurring blurs the area outside the salient area to reduce optical flow. Nie et al. first found that a salient-detection-based dynamic blurring can significantly reduce cybersickness [50]. Lin et al. tested the effect of different central blurring window sizes on cybersickness, but did not find any significant effect [36].

Artificial Vestibular Stimulus Researchers have introduced different vestibular techniques to treat cybersickness. Galvanic vestibular stimulation (GVS) can elicit a vestibular response without physical movement. As a result, researchers have successfully used GVS to mitigate visual-vestibular conflict [23, 64]. Although GVS is a promising technique, it provides unrealistic inertial information to users, making them even more difficult to balance their bodies when visual information in VR is already unrelated to the constraints on the control of the body [27]. Also, GVS is risky to certain populations and difficult to control, which should be used with caution [23, 57]. Another potential way to stimulate the vestibular system is noisy vibration, which can be applied in different ways, such as bone-conductive vibration [57] or floor vibration [29]. In addition, researchers have explored applying force feedback on the user's head using air propulsion jets [39] or padded swing arms [40]. Finally, Lin et al. developed an intentional head motion based locomotion interface to help prevent cybersickness [37].

Rest Frame The Rest Frame Hypothesis is an alternate theory on motion sickness, which claims that humans tend to select things and treat them as stationary references. Whittinghill et al. showed that adding a virtual nose might help reduce cybersickness [74]. Cao et al. proposed dynamic rest frames, where the virtual object used as a rest frame could fade in and out smoothly according to acceleration [9]. They found that the dynamic rest frame did not work as well as the static ones. However, Zielasko et al. found no significant difference with a rest frame added [83].

Geometry Deformation To the best of our knowledge, there are only a few geometry deformation-based techniques that have been proposed to mitigate cybersickness. Lou et al. proposed two deformation methods: one is to compress meshes in the direction of locomotion to reduce the optical flow, and the other is to deform the virtual environment and make the navigation trajectories smoother [42]. However, the authors did not empirically evaluate the effects on cybersickness, and the motivation of this method is fundamentally different than our proposed deformation technique. Chen et al. proposed a space deformation method to help navigate a city [10]. Han et al. introduced Foldable Spaces to redirect users during natural walking using a perceivable transformation [24].

2.3 Uneven Terrain Simulation

In comparison to cybersickness, simulation of uneven terrain such as a slope has not been as extensively explored in the literature. A slope naturally affords acceleration because of gravity. It is difficult to simulate a slope using only visual feedback. Marchal et al. manipulated the motion of the camera to simulate a bump or a hole [44]. Matsumoto et al. proposed a redirected walking technique to simulate uphill and downhill walking by changing the walking distance in a way similar to translation gain [45]. Yamamoto et al. also proposed a way to visually redirect users to feel like they are on a Mobius Strip [81]. Other researchers also tried to use haptic devices to accomplish similar goals [49, 63, 71]. However, navigating

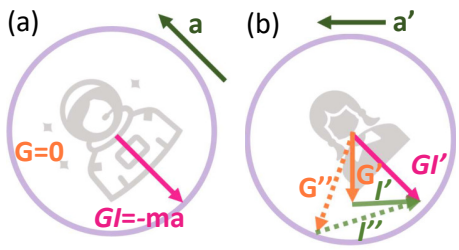

Figure 2: When staying inside a spherical container whose acceleration is a, we assume there is no visual information about orientation or acceleration. The vector of perceived gravito-inertial force is the only information source about motion. (a) When gravity is zero, like in deep space, The inertial force vector alone can specify acceleration because $GI = -ma$. (b) However, gravity is not zero on Earth. Without information on the direction of gravity, we cannot specify the vector of acceleration because there exist multiple potential combinations of different gravity and inertial forces that can add up to the perceived gravito-inertial force.

uneven terrain using existing techniques can increase users' cybersickness [4,16]. Unlike previous works that did not rigorously follow physical rules, in this paper, we simulate a slope using the emergent pattern of both optical and inertial information when accelerating freely on a physical slope.

3 Dynamics and Information

Motion triggers changes in patterns of optical flow (optical information) and gravito-inertial force (inertial information), and humans can discern information about motion from both patterns. Moreover, humans need both optical and inertial information for precise perception. In this section, we will analyze the optical and inertial information available to our perceptual system when moving in different environments. Our analysis in this section will motivate the design of space deformation by utilizing the ambiguity of both optical and inertial information.

3.1 Ambiguity of Inertial Information

The acceleration of our body induces an inertial force that stimulates our vestibular system and provides information about acceleration. An inertial force or pseudo force is a force that an object receives when its motion is described in a non-inertial frame of reference [20]. Inertial forces are always proportional to the object's mass and point away from acceleration. According to the equivalence principle, since there is no physical difference between gravitational and inertial forces, it is impossible to distinguish between them [17]. The vector sum of gravity and inertial force is the gravito-inertial force. As is shown in figure 2, without any knowledge about the direction of gravity, we cannot separate gravity and inertial force from the GIF vector. There exist infinite potential combinations of gravity and inertial force to produce the same GIF. As a result, GIF cannot specify the orientation relative to the Earth independently [26, 43]. For example, in aviation, this phenomenon can result in somatogravic illusion, where pilots will interpret the direction of GIF to be the direction of gravity when accelerating. Consequently, pilots may mistakenly pitch the aircraft down and cause fatal crashes [11]. Due to such ambiguity, our perception system needs other information to achieve precise perception.

On the other hand, GIF is important for body balance because if the body is not supported at its center of mass (GIF vector and ground support are not aligned), a torque will disturb the body's control of stance [20, 60]. The act of orientation is also affected by GIF, because for postural control in the physical world, the direction of balance is always contra-parallel to the direction of GIF vector [66].

3.2 Ambiguity of Optical Information

Optical information can be extracted from the apparent motion of objects caused by the relative movement of the observer through a scene [21]. Gibson et al. first showed that the translation of an observer through a stationary environment produces a radial optical flow pattern. These patterns are specified by the velocity of the observer (V) and the distance from the light source to the observer (D) simultaneously. The mathematical relationship is described in equation 1 [22].

$$\frac{d\delta}{dt} = \frac{V \cdot \sin(\delta)}{D} \tag{1}$$

When approaching a flat surface, the angle of approach, which may vary from zero (parallel locomotion) to 90° (perpendicular locomotion), can affect the optical flow patterns. As a result, we can tell the angle of approach from optical flow. Warren and Hannon's study confirmed that the radial patterns of optical flow could be used to perceive the translational direction of self-motion even under the influence of eye movements [73]. However, since the optical flow field only gives the ratio of the observer's velocity and distance, we cannot fully determine these values using optical information alone [41]. As a result, we can use optical flow to detect the relative change in the velocity, but we need precise knowledge about the sizes of objects in the environment to specify absolute velocity.

The structure of optical information also contains information about orientation. For example, the horizon is perpendicular to the pull of gravity [21, 26]. And stems grow in the opposite direction of gravitational pull [13]. The walls of buildings should also orient towards the direction of gravity to maintain the best stabilization. Neuroscience studies have found evidence that we can pick up information about our orientation visually [26].

3.3 Information in Different Environments

In this subsection, we will analyze and compare the optical and inertial information available in these environments. To simplify our analysis, we assume there is no friction or other kinds of resistance in the environment. Also, the human body is considered rigid. Although this assumption is ideal, it is generalizable to the real world. The body's mass is m, and gravitational acceleration is g.

Standing on A Flat Surface When a human moves at a constant velocity, which might be zero, on a flat surface, the GIF is only the gravity since the inertial force is zero. The support force from the ground is of the same magnitude and opposite direction as gravity. If gravity passes through the object's bottom, it will be balanced. Postural sway will happen when standing still. But the direction of balance will always be the direction of gravity. In this case, the optical flow will also indicate a constant translation velocity.

Accelerate on A Flat Surface When a horizontal force pushes a human to accelerate (figure 3b), the inertial force will not be zero because of acceleration. The direction of GIF becomes tilted, forcing the human to adjust their posture. It is commonly noticed that when a human voluntarily starts to accelerate forward, they will tilt their body forward so that it is aligned with GIF. A similar effect was also found on car drivers [72]. Acceleration can also affect optical flow patterns based on equation 1. In VR, however, we can see this accelerating optical flow pattern without being affected by the inertial force, which may cause cybersickness.

Ski Down A Slope As is shown in figure 3c, when a human is on a slope, the component of gravity along the slope will make them accelerate at a rate of $g\sin\theta$, where θ is the inclining angle of the slope. As a result, GIF is the component of gravity perpendicular to the slope, which is $g\cos\theta$. Since $\cos\theta \approx 1$ when θ is small (e.g. $\cos 5^\circ = 0.996$), the magnitude of GIF is indistinguishable from the magnitude of gravity force. The vestibular system grows on the body and perceives GIF in the body's reference frame. In this case, the

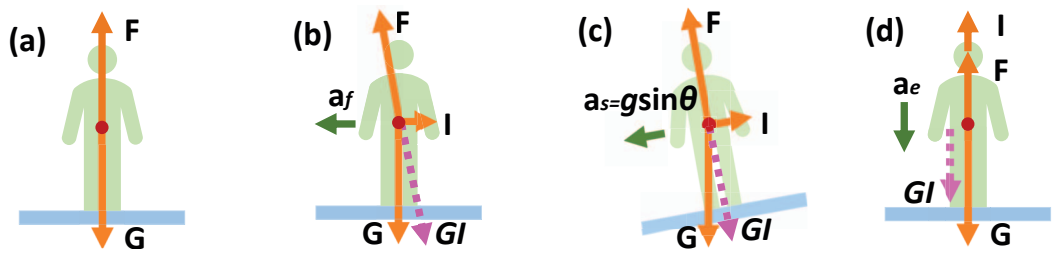

Figure 3: Simplified dynamics of a human standing on different surfaces in their own frame of reference. $G = mg$ is the gravity, F is the sum of external forces, which is ground support only in (a,c,d) or the vector sum of ground support and a horizontal force that pushes the human to accelerate, I is the inertial force, and GI is the gravito-inertial force, which is the vector sum of G and I. The red dot represents the body's center of mass. (a) On a flat surface, ground support fully compensates for gravity. $F = -G$. (b) When a force pushes a human to accelerate at a_f, in the human's reference frame, the inertial force is $-ma_f$. This change in GI can stimulate their vestibular system. (c) On a smooth slope, the human will start to accelerate downhill because of gravity. The acceleration is $a_s = g\sin\theta$, where θ is the slope. Because of acceleration, in the human's frame of reference, there should be an inertial force I pointing uphill. As a result, the direction of GI and F is perpendicular to the slope. $||GI|| = mg\cos\theta$. (d) On an elevator accelerating downwards with an acceleration a_e, the human inside the elevator will experience weightlessness because of inertial force, where $GI = G - ma_e$.

direction of GIF is also perpendicular to the supporting surface in the human's reference frame. As a result, the GIF on a slope has exactly the same relative direction and very similar magnitude as the GIF when we are standing on a flat surface. This ambiguity provides us a chance to simulate a slope and mitigate cybersickness.

Accelerate Downwards Humans will experience weightlessness when accelerating downwards because of inertial force. Given an acceleration of a_e, if $a_e = g - g\cos\theta$, $||GIF|| = mg\cos\theta$. In this case, even the most precise accelerometer will not be able to distinguish the difference between skiing on a slope or accelerating down. This ambiguity further confirms that the vestibular system cannot specify acceleration independently, and there is a cooperation between perceptual systems to achieve accurate motion perception.

4 Space Deformation

As mentioned in section 3.3, if we accelerate freely on a slope, the GIF has the same relative direction and very close magnitude as the gravity we experience when standing on the ground. If we can replicate the structure of a slope visually when the user is accelerating virtually, we can restore the physical relationship between the optical and inertial information available to the user. A slope has two major visual properties in the real world. First, a slope shall always be finite. We can see the end of a slope where the ground's surface changes from tilted to flat. When standing on a slope, downhill objects are more visible while the ground often occludes uphill objects. The steeper the slope, the more obvious this phenomenon is. Second, stationary objects on a slope, like trees or buildings, will tend to orient towards the direction of gravity because it is easier to maintain balance in that way. The slope of the surface is approximately the angle between the ground normal and the direction of gravity indicated by stationary objects. These natural phenomena convey information about the slope of the ground, which can be picked up visually by our perceptual system. Our goal is to replicate this visual stimuli pattern using a geometry transformation.

In this section, we describe a shader-based method to deform the VE in real-time using the visual properties above. We implemented space deformation using an HLSL shader in Unity. A tessellation shader will tessellate the triangles close to the point of view to make the transformed surface smoother, and a geometry shader will perform the proposed geometry transformation at run-time.

4.1 Geometry Transformation

An overview of the proposed space deformation (an affine transformation) is shown in figure 4, and a detailed description of the geometry transformation is provided in algorithm 1. Please note this paper uses a left-handed convention for its coordinate system, which is the same as Unity and Unreal Engine but different from OpenGL. This deformation was invoked when the user accelerated or decelerated virtually. The transformation produces a **ground bending** visual effect in which distant portions of the VE appear to bend up or down (see figure 1). The portions of the VE close to the user will only slightly change orientation, as shown in figure 4d. The skybox also rotates around the user's local x-axis so that it aligns with transformed objects placed infinitely far away.

This algorithm is applied to each vertex in a shader and runs on a GPU. It takes the vertex's world position as input and outputs the updated vertex position to perform the desired deformation. The algorithm defines the following variables that are shared across all

Algorithm 1 The geometry transformation of space deformation

Require: All vectors (capital, bold) are in world space.
Require: All direction vectors are normalized.
Require: The camera's position is already projected to the ground.
$\boldsymbol{V} \leftarrow$ vertex position
$\boldsymbol{C} \leftarrow$ camera position
$\boldsymbol{X} \leftarrow$ camera's left direction (projected to XZ plane)
$\boldsymbol{Y} \leftarrow$ ground normal
$\boldsymbol{Z} \leftarrow$ camera's forward direction (projected to XZ plane)
$\boldsymbol{G_p} \leftarrow$ a point on ground
$l \leftarrow$ slope's length
$\theta \leftarrow$the slope's angle
$Plane\ \boldsymbol{p} = Plane(\boldsymbol{Z}, \boldsymbol{C})$ ▷ $\boldsymbol{p}$ has normal $\boldsymbol{Z}$ and goes through $\boldsymbol{C}$.
$d = \boldsymbol{p}.GetDistanceToPoint(\boldsymbol{V})$
if $d < -0.5l$ **then**
    $\boldsymbol{P}_{down} = \boldsymbol{C} + 0.5l\boldsymbol{Z}$
    $\boldsymbol{V} = \boldsymbol{V} - \boldsymbol{P}_{down}$
    $\boldsymbol{V'} = rotate(\boldsymbol{V}, \boldsymbol{X}, \theta) + \boldsymbol{P}_{down}$ ▷ Rotate $\boldsymbol{V}$ around axis $\boldsymbol{X}$
else if $(d \geq -0.5l)$ and $(d \leq 0.5l)$ **then**
    $\boldsymbol{V}_G = \boldsymbol{V} - dot(\boldsymbol{V} - \boldsymbol{G_p}, \boldsymbol{Y})\boldsymbol{Y}$ ▷ Project $\boldsymbol{V}$ to the ground
    $\boldsymbol{V} = \boldsymbol{V} - \boldsymbol{V}_G$
    $\boldsymbol{V'} = rotate(\boldsymbol{V}, \boldsymbol{X}, \theta) + \boldsymbol{V}_G$
else if $d > 0.5l$ **then**
    $\boldsymbol{P}_{up} = \boldsymbol{C} - 0.5l\boldsymbol{Z}$
    $\boldsymbol{V} = \boldsymbol{V} - \boldsymbol{P}_{up}$
    $\boldsymbol{V'} = rotate(\boldsymbol{V}, \boldsymbol{X}, \theta) + \boldsymbol{P}_{up}$
end if
return $\boldsymbol{V'}$

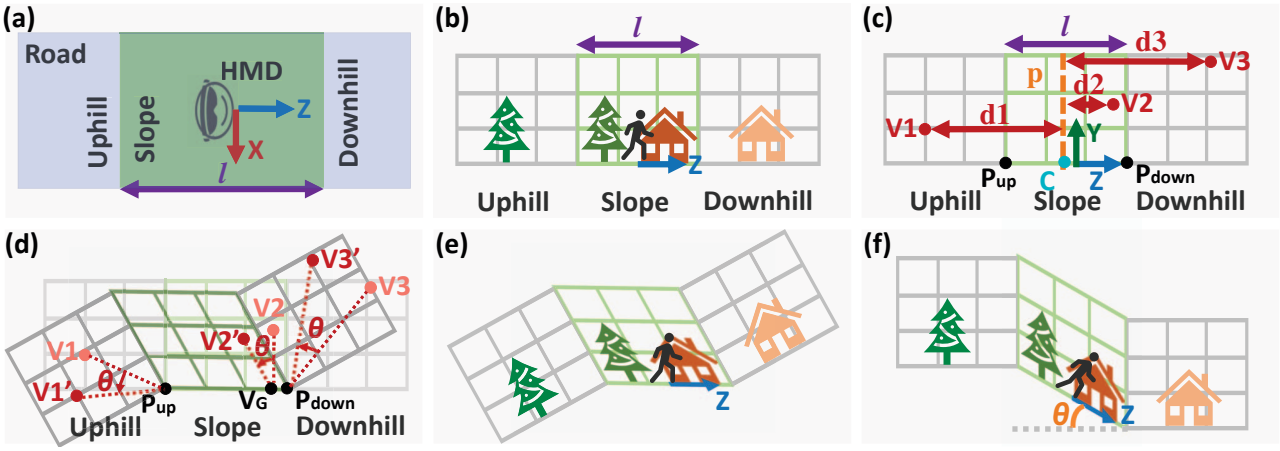

Figure 4: The geometry transformation to simulate a slope. $\boldsymbol{X}$, $\boldsymbol{Y}$ and $\boldsymbol{Z}$ are the HMD (camera)'s left, up and forward directions. $\boldsymbol{C}$ is the camera's position projected to the ground plane. And l is the length of the slope we will simulate. (a) The top-down view of the VE, which is divided into three areas: uphill, slope, and downhill. The camera is in the middle of the slope. (b) The left side view of the VE before deformation. The user is facing and accelerating virtually in $\boldsymbol{Z}$ direction. (c) Given a vertex in the VE, we will first determine which area it belongs to based on its distance d to plane $\boldsymbol{p}$, a plane that has normal $\boldsymbol{Z}$ and goes through $\boldsymbol{C}$. Positions of points $\boldsymbol{P}_{up} = \boldsymbol{C} - 0.5l\boldsymbol{Z}$ and $\boldsymbol{P}_{down} = \boldsymbol{C} + 0.5l\boldsymbol{Z}$ will be used in the next step. (d) If the vertex is in the uphill or downhill area, it should rotate counterclockwise around an axis defined by direction $\boldsymbol{X}$ and a point $\boldsymbol{P}_{up}$ or $\boldsymbol{P}_{down}$. If the vertex is in the slope area, it should rotate counterclockwise around an axis defined by $\boldsymbol{X}$ and its own projection on the ground. (e) An illustration of the VE after transformation. (f) The slope effect we would like to simulate.

vertices in a single frame. The CPU updates their values in each frame when the VR application is running.

Two scalar parameters affect the visual effect after deformation: the slope's length l and the angle of inclination θ. The length l was set to 30 meters. To determine the various parameters used in the study, we conducted extensive pilot testing with multiple users who were encouraged to explore many different combinations of the parameters under the guidance of the experimenter and report the combinations that felt most comfortable. This was done using a spatial menu that allowed testers to dynamically adjust the parameters related to our space deformation implementation. The maximum value of θ was determined by the physical laws in equation 2 such that the slope can afford the desired acceleration a.

$$\theta_{max} = \arcsin\frac{a}{g} \tag{2}$$

Also, five 3D vector parameters affect the position and orientation of the deformation. All these vectors are in world space, and all directions are normalized. $\boldsymbol{C}$ is the camera's projection on the ground. $\boldsymbol{X}$ and $\boldsymbol{Z}$ are the projection of the camera's left and forward direction projected to the horizontal plane. $\boldsymbol{Y}$ is the up direction of the world, which is always $(0,1,0)$. $\boldsymbol{G_p}$ is a point on the ground plane, which can be $(0,0,0)$ when the ground level is 0 for convenience.

4.2 Transition

Bending Time The geometry transformation above was performed gradually when users started virtual acceleration. As described previously, we also determined the time for bending through extensive pilot testing and implemented an asymmetric bending time to balance responsiveness and comfort in the locomotion interface. When users start to accelerate forward, the ground will bend upwards within 0.3 seconds. On reaching the maximum velocity, the acceleration will stop. However, the ground will start to bend back 2 seconds after that and bend back to flat in 1.2 seconds. This delay is intended to make the bending back less obtrusive. When users start decelerating, the ground will bend downwards in 0.3 seconds and bend back in 1.2 seconds when the speed is close to zero.

Angle of Inclination During bending, the angle of inclination θ changes gradually from 0 to θ_{max} or vice versa. The most straightforward way to implement this is to linearly increase θ until it reaches θ_{max}, like equation 3, where Δt is the time from the start of bending to now and t_{bend} is the bending time.

$$\theta = \frac{\Delta t}{t_{bend}}\theta_{max} \tag{3}$$

However, as is shown in equation 4, we further smoothed this process by mapping the linear increase to a triangular function.

$$\theta = 0.5 * \sin\theta_{max} * (\cos((1 + \frac{\Delta t}{t_{bend}}) * \pi) + 1) \tag{4}$$

4.2.1 How to Bend: Tilt And Pinch Effect

One potential limitation of our space deformation technique is its modification to the geometry of the VE. Changes to the VE's geometry when space deformation starts to take place may introduce undesired effects for users. For example, when the ground bends up, users will see the downhill area rotate upwards. Also, objects that are very far away from the point of view, such as the skybox, will rotate around the user. To investigate and minimize this effect, we created two effects and compared them in the user study.

Tilt For this visual effect, the slope's length l is kept constant during bending (see figure 5a). This effect is straightforward and intuitive. However, it could create a rotational self-motion illusion that may potentially induce discomfort. As a result, we also developed the pinch effect, which changes the length of the slope dynamically.

Pinch For the pinch effect, the slope's length changes with the angle of inclination θ (see figure 5b). The length l' is calculated according to equation 5. l is a constant and equals the length of the slope at the end. By changing length, we hope to create a feeling that the user's altitude ($l' \sin\theta$) is a constant during the transition.

$$l' = \frac{\sin\theta_{max}}{\sin\theta}l \tag{5}$$

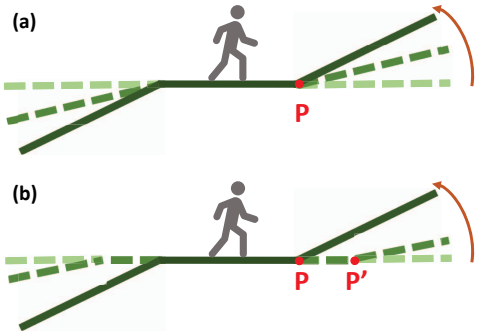

Figure 5: An illustration of both the tilt effect (a) and pinch effect (b). The length of the slope is fixed in the tilt effect, but it changes according to equation 5 in the pinch effect.

5 User Study

5.1 Experiment Design

In this experiment, we evaluate the effectiveness of the proposed geometry transformation during linear acceleration. We conducted a between-subjects study with three conditions: (1) space deformation with the pinch effect, (2) space deformation with the tilt effect, and (3) control with no deformation. The objectives were to investigate the effects on both slope perception and user comfort. We were uncertain about the impact of the transition animations on the user experience, but we hypothesized that the pinch effect may be more comfortable because it does not create rotational motion as strong as the tilt effect. The specific measures and scientific hypotheses are described in further detail in sections 5.6 and 5.7. This study was conducted in our laboratory, and the protocol was reviewed and approved by our University's Institutional Review Board (IRB).

5.2 Participants

A total of 91 participants (41 female) between the ages of 18 and 64 volunteered to participate. Participants were recruited through the university via class announcements and postings to online communities such as Reddit and Discord. The inclusion criteria required participants to be 18 years or older, able to converse in both written and spoken English, able to stand/move without help, have normal or corrected vision, and not pregnant. Four participants (2 male and 2 female) did not finish the study due to equipment failures or personal reasons (not related to cybersickness). 56 participants had no prior experience with VR, and 35 participants had prior experience with VR. All participants were compensated with a $15 gift card.

5.3 Equipment

Participants experienced the virtual environment using an Oculus Quest headset with Oculus Link, which was connected to the PC by a USB 3.0 compatible cable. The headset provides a stereoscopic view with a resolution of 1440 × 1600 per eye, a refresh rate of 72Hz, and a field of view of around 104 degrees. The application was implemented in Unity 2020.3.18f1. The experiment was run on an Intel Core i9-9900K 3.60GHz PC running Windows 10 Pro with 64 GB of RAM and an NVIDIA GeForce RTX 2080 graphics card.

5.4 Virtual Environment

The virtual environment was a city that contained 20 square 18×18 meter blocks (see figure 6). The width of the streets was approximately 6 meters. We placed stop signs on the road so that participants have to accelerate and stop frequently. Combined audio/visual guidance cues were used in the navigation task to provide instructions. When approaching a stop sign, there would be an audio instruction saying 'stop.' At each turning point, the participant would hear another audio instruction saying 'turn left' or 'turn right,' and a yellow arrow indicating the same turning direction would appear.

Figure 6: The top view of the virtual environment in this study.

The study used view-directed steering as the locomotion interface. Participants were instructed to stand still during the experiment and navigate the VE using a controller's joystick. They have to turn by rotating their whole body physically. The max velocity was 2.5 meters per second. When participants pushed the joystick, the velocity would accelerate smoothly at a rate of $1m/s^2$, and it would smoothly decelerate at the same rate when the joystick was released.

5.5 Procedure

At the beginning of the study session, the experimenter received oral confirmation that the participant met all of the inclusion criteria, introduced the task, showed the participant how to use the controller, and reviewed the IRB-approved information sheet. Participants were informed that they were asked to report their discomfort level at the end of each trial and that they should stop the VR experience if they were feeling sick. Before the participant entered the virtual space, they completed the SSQ pre-questionnaire on a PC.

Participants remained standing during the VR experience. For each trial, they were given one of the predefined virtual paths that passed through the VE. Participants could virtually move forward using the controller and were instructed to stop or turn only after they heard the corresponding audio instruction. At each stop sign, participants needed to stop for three seconds before they could start moving forward again. Once the participant put on the headset, the experimenter instructed the participant to complete a one-minute practice trial with four stop signs. After completing the practice, participants then completed 10 experimental trials, each of which was designed to take approximately two minutes, resulting in an overall VR exposure time of about 21 minutes. At the end of each trial, participants were asked to rate their discomfort level on a 0 to 10 scale using a slider before they went to the next trial. The VR experience terminated when the participant finished all the trials or whenever they entered a discomfort score of 10. In the post-study questionnaire, participants completed the SSQ post-questionnaire, a subjective feedback questionnaire, and a demographic questionnaire. The entire experiment was designed to take about 30-40 minutes to complete, including all questionnaires.

5.6 Measures

We collected the following data to evaluate the effect of space deformation on people's perception in VR.

Cybersickness The participants' level of cybersickness was measured using the Simulator Sickness Questionnaire (SSQ). The questionnaire was administered immediately before and after the VR experience. For each participant, we calculated the total severity scores and then computed the delta to evaluate changes in cybersickness-related symptoms.

Discomfort Scores Discomfort scores were collected after every two-minute trial by prompting the participants to self-report their level of discomfort. Following Fernandes and Feiner's [19] approach, we calculated two variables from the discomfort scores: the *Average Discomfort Score (ADS)* and the *Relative Discomfort Score (RDS)* using the following equations:

$$ADS = \frac{\sum_{0 \le i \le t_{stop}} DS_i}{N} \tag{6}$$

$$RDS = \frac{\sum_{0 \le i \le t_{stop}} DS_i + (t_{max} - t_{stop} + 1) DS_{stop}}{t_{max}} \tag{7}$$

The duration of the VR experience for each participant was t_{stop}. The longest duration across all participants was t_{max}. The last discomfort score at t_{stop} was DS_{stop}. If a participant terminated before t_{max}, their DS_{stop} was set to 10 and was repeated for all subsequent trials.

Objective Measures We measured the time each participant took to finish the task because the locomotion task terminated when the participant was feeling severe discomfort. The VR application recorded the duration of each trial by measuring the time between they first started moving and they stopped at the end of the trial. We also recorded the position and orientation tracking data from the headset to explore the effects of the space deformation techniques on participants' movement and posture.

Subjective Experience The effectiveness of the space deformation technique on slope simulation was primarily assessed through two real questions embedded in a list of decoy phenomena, similar to the approach used in several previous studies [19, 56, 69]. Participants were asked to rate each of the following statements on a scale of 1="did not notice or did not happen" to 7="very obvious." The following seven statements were provided to the participants, of which only the primary outcome measurements (questions 3 and 6) are related to space deformation.

- I saw the virtual environment get smaller or larger.
- I saw the virtual environment flicker.
- *I felt like the virtual environment was bending.*
- I saw something in the virtual environment had changed color.
- I felt like my field of view was changing in size.
- *I felt like I was on a slope.*
- I saw the virtual environment get brighter or dimmer.

The first target question '*I felt like the virtual environment was bending*' was fairly obvious when space deformation is active because it is a perceivable transformation. We used this question as a baseline for an obvious phenomenon. The second target question '*I felt like I was on a slope*' was used to measure participants' subjective perception on walking on a slope. If space deformation created a feeling of being on a slope successfully, the rating for this question should also be higher than the decoy questions. After the subjective experience questionnaires, we also included free-response questions to gather qualitative feedback about the space deformation technique and its impact on user comfort.

5.7 Hypotheses

We defined the following scientific hypotheses to evaluate the effects of space deformation techniques on the user experience.

- **H1.A**: Participants would report lower delta SSQ scores in the space deformation conditions compared to the control.
- **H1.B**: Participants would report lower delta SSQ scores in the Pinch condition compared to the Tilt condition.
- **H2.A**: Participants would report lower discomfort scores in the space deformation conditions compared to the control.
- **H2.B**: Participants would report lower discomfort scores in the Pinch condition compared to the Tilt condition.

Figure 7: Participants stopped at each stop sign. When they need to turn, the road in front of them is blocked by a barricade. After they reached a full stop, they heard an audio instruction and saw a yellow arrow that indicated the same turning direction pop up.

- **H3**: Participants' slope perception ratings would be higher in the space deformation conditions compared to the control.
- **H4**: Participants' pitch head orientation would be correlated with discomfort scores in the space deformation conditions.

We formulated H4 after we reviewed participants' subjective feedback when the study finished (see section 7.1). Many participants in the Pinch and Tilt conditions mentioned that the rotation of objects, especially those that were far away from the skybox, was making them feel uncomfortable. However, multiple participants also reported adapting to space deformation after a few trials. Based on these comments, we suspected that participants who tended to look more on the ground would be more comfortable because the ground around the point of view did not change its shape during the transition. It should be noted that we defined hypothesis H4 before conducting analyses of the quantitative data. Because our experiment equipment does not support eye tracking, we used participants' head orientation data to approximate their gaze direction.

6 Results

Among a total of 87 participants, four participants in the Control condition (3 female) terminated before finishing all of the trials. No participants terminated early in the Pinch and Tilt conditions. We first conducted Shapiro-Wilk tests for all variables and found that none of them were normally distributed. For the non-parametric data, we used Kruskal-Wallis tests to analyze differences between the three conditions (Control, Pinch, Tilt) and reported descriptive statistics as median (*Mdn*) and interquartile range (*IQR*). Statistical tests assumed a significance value of $\alpha = .05$. When a Kruskal-Wallis test rejected the null hypothesis, we conducted the post-hoc analysis using pairwise Conover tests with a Holm-Bonferroni correction.

SSQ Results of SSQ scores are shown in figure 8. Analysis results of the differences between the pre- and post-SSQ scores indicated no significant difference among the Control ($Mdn = 18.70$, $IQR = 33.66$), Pinch ($Mdn = 22.44$, $IQR = 26.18$) and Tilt conditions ($Mdn = 22.44$, $IQR = 22.44$), $\chi^2(2) = 0.32$, $p = .85$. This result does not support H1.A or H1.B.

Discomfort Scores Results for average and relative discomfort scores are shown in figure 9. In our experiment, the longest time a participant spent in VR was 1818 seconds (30.3 mins). However, this participant was an extreme outlier because their duration was over three times the *SD* (= 147.46) away from the *Mean* (= 1347.78). Therefore, we set t_{max} to 1608 seconds, the second longest duration. Analysis results of ADS indicated no significant difference among the Control ($Mdn = 2.19$, $IQR = 2.06$), Pinch ($Mdn = 1.83$, $IQR = 2.17$), and Tilt conditions ($Mdn = 1.93$, $IQR = 2.50$), $\chi^2(2) = 0.629$, $p = .73$. The RDS results also indicated no significant difference among the Control ($Mdn = 2.16$, $IQR = 2.12$), Pinch ($Mdn = 2.07$, $IQR = 2.85$), and Tilt conditions ($Mdn = 1.92$, $IQR = 2.60$), $\chi^2(2) = 0.478$, $p = .78$. These results do not support H2.A or H2.B.

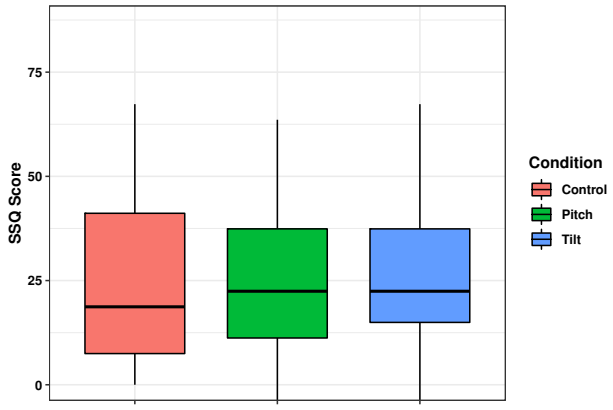

Figure 8: Box plots of the delta SSQ scores for each condition.

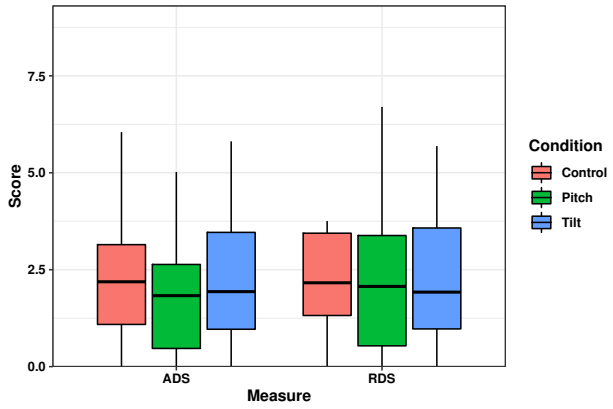

Figure 9: Box plots of average discomfort scores (ADS) and relative discomfort scores (RDS) for each condition.

Slope Perception Figure 10 shows how our two target questions compare with the decoy questions in their average ratings. Median ratings for the decoy questions ranged from 0 to 2 as a result of random guessing, which consists with previous findings [19,69]. The analysis for the first target ('bending') question revealed a significant difference among the three conditions, $\chi^2(2) = 44.505$, $p < .001$. Post-hoc analysis indicated that the 'bending' question was rated as more obvious in the Pinch condition ($Mdn = 7$, $IQR = 4$) compared to the Control condition ($Mdn = 1$, $IQR = 0$), $p < .001$. The Tilt condition ($Mdn = 7$, $IQR = 1$) was also associated with higher ratings compared to the Control condition, $p < .001$. There was no significant difference between the Pinch condition and the Tilt condition, $p = 0.119$. This result is unsurprising because space deformation was not designed to be imperceptible.

The analysis for the second target ('slope') question revealed a significant difference among the three conditions, $\chi^2(2) = 45.042$, $p < .001$. Post-hoc analysis indicated that the 'slope' question was rated as more obvious in the Pinch condition ($Mdn = 7$, $IQR = 2$) compared to the Control condition ($Mdn = 1$, $IQR = 0$), $p < .001$. The Tilt condition ($Mdn = 7$, $IQR = 3$) was also associated with higher ratings compared to the Control condition, $p < .001$. There was no significant difference between the Pinch condition and the Tilt condition, $p = 0.662$. These results suggest that both space deformation effects elicited a very strong feeling of being on a slope while participants were physically standing still on flat ground using artificial optical stimulus only, which supports H3.

Head Orientation To analyze the relationship between pitch head orientation during ground bending and participants' discomfort scores, we collected frames with nonzero acceleration and averaged the pitch angle. Positive angles corresponded to view directions below the horizon line, and negative angles corresponded to view directions above the horizon line. We compared participants' average pitch rotation with RDS ratings to investigate if a systematic relationship exists between head orientation and cybersickness. This analysis was conducted separately for each of the three conditions. For the Pinch condition, there was a negative correlation, $r(27) = -.374$, $p = 0.046$, indicating that downward-pointing head rotation angles were associated with lower discomfort scores. No significant correlation was observed in the Control condition, $r(27) = -.091$, $p = 0.637$), and the Tilt condition, $r(27) = .018$, $p = 0.925$. These results support H4 for the pinch effect but not for the tilt effect.

7 Discussion

Cybersickness and Discomfort We did not observe any significant differences in discomfort or cybersickness, so we cannot draw any definitive conclusions. However, it is possible that the gravito-inertial physics simulation could have provided some benefits that were effectively canceled out by discomfort induced by the dynamic ground bending visual effect. The vast majority of participants' comments suggest that space deformation made them uncomfortable, and only 5 out of 58 participants across both of these conditions reported that it made them feel more comfortable in their qualitative feedback. To describe the sensation during ground bending, participants used words like "dizzy," "disoriented," "distracting," and "difficult to balance." Other participants also commented ground bending is something unnatural, weird, or unrealistic. Although we had expected the visual effect to cause some minor side effects, this was initially viewed as a potentially worthwhile tradeoff if it could reduce cybersickness during linear acceleration. However, the side effect was stronger than our expectations, and the cybersickness induced by linear acceleration is generally less severe than virtual turning. Additionally, SSQ scores were relatively low overall for a 20 minute VR experience that uses virtual locomotion, and these data suggest a potential floor effect. Interestingly, participants' SSQ and discomfort scores were noticeably lower than those observed during pilot testing. However, the variability of these data were larger than our expectation based on a similar previous study [77]. For RDS, if the the smallest reduction of interest is 1.0 and its standard deviation is 2.5, we calculated that the effect size (Cohen's *d*) would be .18. A post-hoc power analysis using G*Power [18] showed that this would provide a statistical power of .32. Due to these factors, we believe that there was little opportunity for the current implementation to simulate the gravito-intertial physics to provide a benefit, and so the general viability of this approach for cybersickness reduction remains an open question.

Slope Simulation The accelerating optical flow, changes to the ground and stationary objects' orientation, and the direction of GIF stimulus contributed together to create a realistic feeling of being on a slope. Ratings on the embedded questions indicated that space deformation induced this feeling strongly even though participants were standing on a flat surface. In the qualitative feedback, many participants expressed a feeling of being on a slope, such as, "*It ... made me feel like I was a ball roling [sic] down a hill/slope*," "*I felt like I was running on a slope,*" and "*It resembled how descending or ascending real roads feel mentally.*" Other participants reported a feeling of falling forward, such as, "*It felt like the ground I was on was tipping me forward,*" and "*It felt like you were going to slide down or fall.*" For some participants, this feeling even "*makes me feel like I'm being dragged and pushed*' and "*had an almost acceleration/deceleration feel.*" Surprisingly, one participant even reported that their feet were sore because they felt like they were on a slope. In the future, it would be interesting to compare space deformation

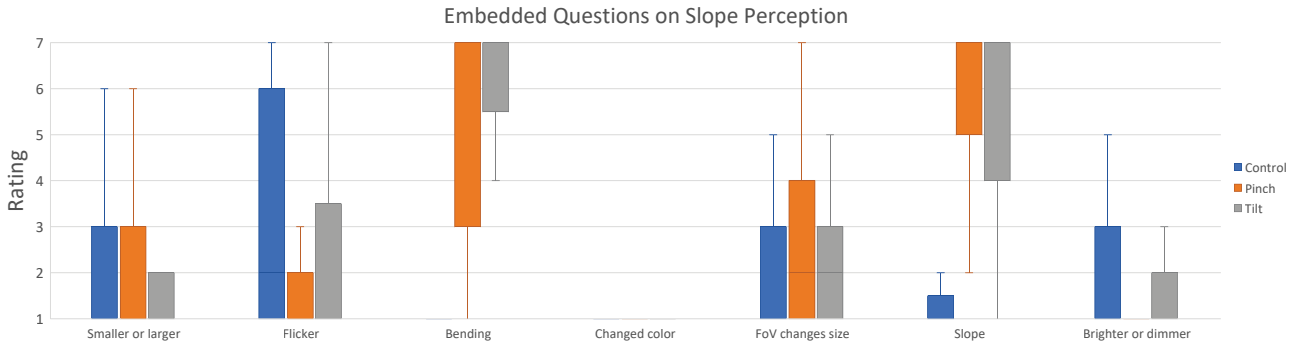

Figure 10: Box plots of the slope perception ratings embedded in multiple decoy questions. A higher rating means the statement is more obvious. Participants reported significantly higher ratings of being on a slope in the Pinch and Tilt conditions compared to the Control.

with other previously proposed slope simulation techniques [44]. For developers, space deformation can be triggered when the user has entered the slope area, and the user's camera will start to accelerate at the same time. Developers can choose to deform the VE gradually. Or they might be able to deform the VE instantly during saccades or blinks if the user' equipment allows so that the changes are less noticeable because of change blindness [33, 70].

Adaptation The correlation between participants' RDS and their heads' pitch orientation suggests the existence of an adaptation strategy to space deformation. One potential explanation is that participants who tend to look more at the ground are less affected by the ground bending because the sky and bending ground are less visible in the users' field of view. The ground meshes that are close to the user remain flat when the ground bends up, which could serve as a rest frame for users. The pinch effect breaks the integrity of the ground that bends up and does not produce a rotational feeling as the tilt effect does. As a result, when the ground bending goes to the peripheral region, the pinch effect will be less provocative than the tilt effect. That could potentially explain why the correlation only happened in the Pinch condition. Although this is a suggestive result in favor of the pinch effect, it is not possible to draw any definitive conclusions from these data. Additionally, we used pitch orientation as an approximation for gaze direction, and further studies are needed to more thoroughly investigate this using eye tracking data.

Limitations and Future Work Aside from discomfort, we identified several limitations for using current space deformation implementation in a continuous locomotion interface. First, the direction of the slope is fixed once the ground bends up. Changing the direction of the slope could induce more discomfort, and we have therefore made the direction fixed in our implementation. However, when users change their head direction, their acceleration direction will be different from the direction of the slope. Second, in the current implementation, ground bending happens too frequently, and participants found this distracting. When users push the joystick to start moving, they will first see the ground bend up to simulate a downhill slope, then bend back to flat after reaching the maximum velocity. Because this also occurs during deceleration, users will see the ground bending four times for each complete translation. One participant explicitly stated that it "*happened too often and not subtly*." It may be possible to explore alternative implementations that can apply ground bending less frequently and for longer periods of time. Third, the current implementation requires a reasonably long accelerating time ($\geq$ 1 second). If the acceleration is discontinuous instead of gradual, there will not be enough time to bend the ground, and the maximum acceleration is also limited by the magnitude of gravity and the largest slope angle we could simulate in a comfortable way. Finally, space deformation applies a shear transformation that does not geometrically preserve right angles, which could result in objects that appear unusual. In summary, these factors currently limit the flexibility of space deformation, although it may be possible to address some of them in future work.

When we designed the current space deformation technique, we focused more on providing a realistic slope illusion. As a result, we implemented the ground bending to allow users to see the downhill area of the slope because, as is mentioned in section 4, a slope should always be finite. However, the orientation of stationary objects on the ground alone (the transformation to the slope area in figure 4d) is also providing information about the direction of gravity. If we only manipulate objects' orientation while not bending the ground and rotating the skybox, it is possible that this could mitigate cybersickness without inducing extra discomfort from the dynamic visual effect. Although this change would likely give users a weaker feeling of being on a slope, we believe it could still affect their perception subconsciously. Additionally, space deformation could potentially be applied using a longer slope length so that the ground bending effect is less visually intrusive.

In our study, we only explored the use of space deformation in linear transformation. However, this approach also has the potential to simulate a banking turn during virtual turning when the translation velocity is non-zero (traveling along a curve). This implementation might have better performance because it will only bend the ground twice during every turn instead of four times per translation. Also, virtual turning induces more severe cybersickness; therefore, the potential benefits might present a more favorable trade-off.

8 Conclusion

In this paper, we introduced and evaluated space deformation, a novel way to simulate slopes in VR using optical information with inertial information also taken into consideration. We integrated space deformation into a continuous locomotion interface to study its effects on both cybersickness and slope perception. Space deformation successfully induced strong feelings of being on a slope. However, we did not find any significant effects on cybersickness and discomfort. In general, these results contribute to the knowledge of human perception and provide several useful insights for future design iterations. We believe this slope simulation approach can potentially be used to provide novel virtual reality experiences that are not constrained by walking only on a flat surface.

Acknowledgments

The authors would like to thank Victoria Interrante, Courtney Hutton Pospick, Thomas Stoffregen, Mary C. Whitton, and Danhua Zhang for their assistance with this research. This material is based upon work supported by the National Science Foundation under Grant No. 1901423.

REFERENCES

[1] I. B. Adhanom, M. Al-Zayer, P. Macneilage, and E. Folmer. Field-of-view restriction to reduce vr sickness does not impede spatial learning in women. *ACM Transactions on Applied Perception*, 18(2), 2021.

[2] I. B. Adhanom, N. Navarro Griffin, P. MacNeilage, and E. Folmer. The effect of a foveated field-of-view restrictor on vr sickness. In *2020 IEEE Conference on Virtual Reality and 3D User Interfaces (VR)*, pp. 645–652. IEEE, 3 2020.

[3] M. Al Zayer, I. B. Adhanom, P. MacNeilage, and E. Folmer. The effect of field-of-view restriction on sex bias in vr sickness and spatial navigation performance. In *Proceedings of the 2019 CHI Conference on Human Factors in Computing Systems*, pp. 1–12. ACM, New York, NY, USA, 5 2019.

[4] S. Ang and J. Quarles. You're in for a bumpy ride! uneven terrain increases cybersickness while navigating with head mounted displays. In *2022 IEEE Conference on Virtual Reality and 3D User Interfaces (VR)*, pp. 428–435. IEEE, 3 2022.

[5] D. E. Angelaki, A. G. Shaikh, A. M. Green, and J. D. Dickman. Neurons compute internal models of the physical laws of motion. *Nature*, 430(6999):560–564, 7 2004.

[6] B. Arcioni, S. Palmisano, D. Apthorp, and J. Kim. Postural stability predicts the likelihood of cybersickness in active hmd-based virtual reality. *Displays*, 58(October):3–11, 2019.

[7] M. Bolas, J. A. Jones, I. McDowall, and E. Suma. Dynamic field of view throttling as a means of improving user experience in head mounted virtual environments, 2014.

[8] D. Bowman, D. Koller, and L. Hodges. Travel in immersive virtual environments: an evaluation of viewpoint motion control techniques. In *Proceedings of IEEE 1997 Annual International Symposium on Virtual Reality*, pp. 45–52. IEEE Comput. Soc. Press.

[9] Z. Cao, J. Jerald, and R. Kopper. Visually-induced motion sickness reduction via static and dynamic rest frames. *2018 IEEE Conference on Virtual Reality and 3D User Interfaces (VR)*, pp. 105–112, 2018.

[10] S. Chen, F. Miranda, N. Ferreira, M. Lage, H. Doraiswamy, C. Brenner, C. Defanti, M. Koutsoubis, L. Wilson, K. Perlin, and C. T. Silva. Urbanrama: Navigating cities in virtual reality. *IEEE Transactions on Visualization and Computer Graphics*, pp. 1–1, 2021.

[11] B. Cheung, K. Money, H. Wright, and W. Bateman. Spatial disorientation-implicated accidents in canadian forces, 1982-92. *Aviation, space, and environmental medicine*, 66(6):579–85, 6 1995.

[12] J. Cummings and J. Bailenson. How immersive is enough? a meta-analysis of the effect of immersive technology on user presence. *Media Psychology*, 19:1–38, 5 2015.

[13] C. Darwin and F. Darwin. *The power of movement in plants*. D. Appleton, 1896.

[14] M. S. Dennison and M. D'Zmura. Cybersickness without the wobble: Experimental results speak against postural instability theory. *Applied Ergonomics*, 58:215–223, 2017.

[15] M. S. Dennison, A. Z. Wisti, and M. D'Zmura. Use of physiological signals to predict cybersickness. *Displays*, 44:42–52, 2016.

[16] J. L. Dorado and P. A. Figueroa. Ramps are better than stairs to reduce cybersickness in applications based on a hmd and a gamepad. *2014 IEEE Symposium on 3D User Interfaces (3DUI)*, pp. 47–50, 2014.

[17] A. Einstein. Über das relativitätsprinzip und die aus demselben gezogenen folgerungen. *Jahrb. Radioaktivität Elektronik*, 4:411–462, 1907.

[18] F. Faul, E. Erdfelder, A. Buchner, and A.-G. Lang. Statistical power analyses using g*power 3.1: Tests for correlation and regression analyses. *Behavior Research Methods*, 41:1149–1160, 11 2009.

[19] A. S. Fernandes and S. K. Feiner. Combating vr sickness through subtle dynamic field-of-view modification. *2016 IEEE Symposium on 3D User Interfaces (3DUI)*, pp. 201–210, 2016.

[20] R. P. Feynman, R. B. Leighton, M. Sands, and E. M. Hafner. The feynman lectures on physics; vol. i. *American Journal of Physics*, 33(9):750–752, 9 1965.

[21] J. J. Gibson. *The Ecological Approach to Visual Perception*. Psychology Press, 11 1979.

[22] J. J. Gibson, P. Olum, and F. Rosenblatt. Parallax and perspective during aircraft landings. *The American Journal of Psychology*, 68(3):372, 9 1955.

[23] C. Groth, J.-P. Tauscher, N. Heesen, M. Hattenbach, S. Castillo, and M. Magnor. Omnidirectional galvanic vestibular stimulation in virtual reality. *IEEE Transactions on Visualization and Computer Graphics*, 28(5):2234–2244, 2022.

[24] J. Han, A. V. Moere, and A. L. Simeone. Foldable spaces: An overt redirection approach for natural walking in virtual reality. In *2022 IEEE Conference on Virtual Reality and 3D User Interfaces (VR)*, pp. 167–175, 2022.

[25] L. J. Hettinger and G. E. Riccio. Visually induced motion sickness in virtual environments. *Presence: Teleoperators and Virtual Environments*, 1(3):306–310, 1 1992.

[26] I. P. Howard. *Human visual orientation*. Wiley, New York, 1982.

[27] J. T. Inglis, C. L. Shupert, F. Hlavacka, and F. B. Horak. Effect of galvanic vestibular stimulation on human postural responses during support surface translations. *Journal of Neurophysiology*, 73(2):896–901, 2 1995.

[28] R. Islam, K. Desai, and J. Quarles. Cybersickness prediction from integrated hmd's sensors: A multimodal deep fusion approach using eye-tracking and head-tracking data. *Proceedings - 2021 IEEE International Symposium on Mixed and Augmented Reality, ISMAR 2021*, (August):31–40, 2021.

[29] S. Jung, R. Li, R. McKee, M. C. Whitton, and R. W. Lindeman. Floor-vibration vr: Mitigating cybersickness using whole-body tactile stimuli in highly realistic vehicle driving experiences. *IEEE Transactions on Visualization and Computer Graphics*, 27(5):2669–2680, 2021.

[30] R. S. Kennedy, N. E. Lane, K. S. Berbaum, and M. G. Lilienthal. Simulator sickness questionnaire: An enhanced method for quantifying simulator sickness. *The International Journal of Aviation Psychology*, 3(3):203–220, 7 1993.

[31] B. Keshavarz and H. Hecht. Validating an efficient method to quantify motion sickness. *Human Factors: The Journal of the Human Factors and Ergonomics Society*, 53(4):415–426, 8 2011.

[32] J. R. Lackner. Motion sickness: more than nausea and vomiting. *Experimental Brain Research*, 232(8):2493–2510, 8 2014.

[33] E. Langbehn, F. Steinicke, M. Lappe, G. F. Welch, and G. Bruder. In the blink of an eye: Leveraging blink-induced suppression for imperceptible position and orientation redirection in virtual reality. *ACM Trans. Graph.*, 37(4), jul 2018.

[34] J. J. LaViola. A discussion of cybersickness in virtual environments. *ACM SIGCHI Bulletin*, 32(1):47–56, 2000.

[35] D. Lee and J. Lishman. Visual proprioceptive control of stance. *Journal of Human Movement Studies*, 1(April):87–95, 1975.

[36] Y.-X. Lin, R. Venkatakrishnan, R. Venkatakrishnan, E. Ebrahimi, W.-C. Lin, and S. V. Babu. How the presence and size of static peripheral blur affects cybersickness in virtual reality. *ACM Transactions on Applied Perception*, 17(4):1–18, 10 2020.

[37] Z. Lin, X. Gu, S. Li, Z. Hu, and G. Wang. Intentional head-motion assisted locomotion for reducing cybersickness. *IEEE Transactions on Visualization and Computer Graphics*, 2626(c):1–14, 2022.

[38] S. Litleskare. The relationship between postural stability and cybersickness: It's complicated – an experimental trial assessing practical implications of cybersickness etiology. *Physiology & Behavior*, 236:113422, 2021.

[39] S. H. Liu, P. C. Yen, Y. H. Mao, Y. H. Lin, E. Chandra, and M. Y. Chen. Headblaster: A wearable approach to simulating motion perception using head-mounted air propulsion jets. *ACM Transactions on Graphics*, 39(4):1–12, 2020.

[40] S.-H. Liu, N.-H. Yu, L. Chan, Y.-H. Peng, W.-Z. Sun, and M. Y. Chen. Phantomlegs: Reducing virtual reality sickness using head-worn haptic devices. In *2019 IEEE Conference on Virtual Reality and 3D User Interfaces (VR)*, pp. 817–826. IEEE, 3 2019.

[41] H. C. Longuet-Higgins. The visual ambiguity of a moving plane. *Proceedings of the Royal Society of London. Series B. Biological Sciences*, 223(1231):165–175, 12 1984.

[42] R. Lou, R. H. Y. So, and D. Bechmann. Geometric deformation for reducing optic flow and cybersickness dose value in vr. In B. Sauvage and J. Hasic-Telalovic, eds., *Eurographics 2022 - Posters*. The Eurographics Association, 2022.

[43] P. R. MacNeilage, M. S. Banks, D. R. Berger, and H. H. Bülthoff. A bayesian model of the disambiguation of gravitoinertial force by visual

cues. *Experimental Brain Research*, 179(2):263–290, 5 2007.

[44] M. Marchal, A. Lecuyer, G. Cirio, L. Bonnet, and M. Emily. Walking up and down in immersive virtual worlds: Novel interactive techniques based on visual feedback. In *2010 IEEE Symposium on 3D User Interfaces (3DUI)*, pp. 19–26. IEEE, 3 2010.

[45] K. Matsumoto, T. Narumi, T. Tanikawa, and M. Hirose. Walking uphill and downhill. In *ACM SIGGRAPH 2017 Posters*, pp. 1–2. ACM, New York, NY, USA, 7 2017.

[46] K. Moghadam, C. Banigan, and E. D. Ragan. Scene transitions and teleportation in virtual reality and the implications for spatial awareness and sickness. *IEEE Transactions on Visualization and Computer Graphics*, 26(6):2273–2287, 6 2020.

[47] J. D. Moss and E. R. Muth. Characteristics of head-mounted displays and their effects on simulator sickness. *Human Factors: The Journal of the Human Factors and Ergonomics Society*, 53(3):308–319, 6 2011.

[48] J. Munafo, M. Diedrick, and T. A. Stoffregen. The virtual reality head-mounted display oculus rift induces motion sickness and is sexist in its effects. *Experimental Brain Research*, 235(3):889–901, 3 2017.

[49] R. Nagao, K. Matsumoto, T. Narumi, T. Tanikawa, and M. Hirose. Ascending and descending in virtual reality: Simple and safe system using passive haptics. *IEEE Transactions on Visualization and Computer Graphics*, 24(4):1584–1593, 4 2018.

[50] G. Y. Nie, H. B. L. Duh, Y. Liu, and Y. Wang. Analysis on mitigation of visually induced motion sickness by applying dynamical blurring on a user's retina. *IEEE Transactions on Visualization and Computer Graphics*, 26(8):2535–2545, 2020.

[51] N. Norouzi, G. Bruder, and G. Welch. Assessing vignetting as a means to reduce vr sickness during amplified head rotations. In *Proceedings of the 15th ACM Symposium on Applied Perception*, SAP '18. ACM, New York, NY, USA, 2018.

[52] C. M. Oman. A heuristic mathematical model for the dynamics of sensory conflict and motion sickness. *Acta Oto-Laryngologica*, 94(sup392):4–44, 1 1982.

[53] C. M. Oman. Motion sickness: a synthesis and evaluation of the sensory conflict theory. *Canadian Journal of Physiology and Pharmacology*, 68(2):294–303, 2 1990.

[54] S. Palmisano, B. Arcioni, and P. J. Stapley. Predicting vection and visually induced motion sickness based on spontaneous postural activity. *Experimental Brain Research*, 236(1):315–329, 2018.

[55] R. Patterson, M. D. Winterbottom, and B. J. Pierce. Perceptual issues in the use of head-mounted visual displays. *Human Factors: The Journal of the Human Factors and Ergonomics Society*, 48(3):555–573, 9 2006.

[56] T. C. Peck, M. C. Whitton, and H. Fuchs. Evaluation of reorientation techniques for walking in large virtual environments. In *2008 IEEE Virtual Reality Conference*, pp. 121–127. IEEE, 3 2008.

[57] Y.-H. Peng, C. Yu, S.-H. Liu, C.-W. Wang, P. Taele, N.-H. Yu, and M. Y. Chen. Walkingvibe: Reducing virtual reality sickness and improving realism while walking in vr using unobtrusive head-mounted vibrotactile feedback. CHI '20, p. 1–12. Association for Computing Machinery, New York, NY, USA, 2020. doi: 10.1145/3313831.3376847

[58] J. T. Reason and J. J. Brand. *Motion sickness*. Academic Press, London; New York, 1975.

[59] L. Rebenitsch and C. Owen. Individual variation in susceptibility to cybersickness. *UIST 2014 - Proceedings of the 27th Annual ACM Symposium on User Interface Software and Technology*, pp. 309–318, 2014.

[60] G. E. Riccio and T. A. Stoffregen. Affordances as constraints on the control of stance. *Human Movement Science*, 7(2-4):265–300, 10 1988.

[61] G. E. Riccio and T. A. Stoffregen. An ecological theory of motion sickness and postural instability. *Ecological Psychology*, 3(3):195–240, 1991.

[62] D. Risi and S. Palmisano. Effects of postural stability, active control, exposure duration and repeated exposures on hmd induced cybersickness. *Displays*, 60:9–17, 2019.

[63] D. Schmidt, R. Kovacs, V. Mehta, U. Umapathi, S. Köhler, L.-P. Cheng, and P. Baudisch. Level-ups: Motorized stilts that simulate stair steps in virtual reality. In *Proceedings of the 33rd Annual ACM Conference on Human Factors in Computing Systems*, vol. 14, pp. 2157–2160. ACM, New York, NY, USA, 4 2015.

[64] M. Sra, A. Jain, and P. Maes. Adding proprioceptive feedback to virtual reality experiences using galvanic vestibular stimulation. In *Proceedings of the 2019 CHI Conference on Human Factors in Computing Systems*, pp. 1–14. ACM, New York, NY, USA, 5 2019.

[65] K. Stanney, B. D. Lawson, B. Rokers, M. Dennison, C. Fidopiastis, T. Stoffregen, S. Weech, and J. M. Fulvio. Identifying causes of and solutions for cybersickness in immersive technology: Reformulation of a research and development agenda. *International Journal of Human–Computer Interaction*, 36(19):1783–1803, 11 2020.

[66] T. A. Stoffregen and G. E. Riccio. An ecological theory of orientation and the vestibular system. *Psychological Review*, 95(1):3–14, 1988.

[67] T. A. Stoffregen and L. J. Smart. Postural instability precedes motion sickness. *Brain Research Bulletin*, 47(5):437–448, 1998.

[68] E. Suma, S. Finkelstein, M. Reid, S. Babu, A. Ulinski, and L. F. Hodges. Evaluation of the cognitive effects of travel technique in complex real and virtual environments. *IEEE Transactions on Visualization and Computer Graphics*, 16(4):690–702, 2010.

[69] E. A. Suma, S. Clark, D. Krum, S. Finkelstein, M. Bolas, and Z. Warte. Leveraging change blindness for redirection in virtual environments. In *2011 IEEE Virtual Reality Conference*, pp. 159–166. IEEE, 3 2011.

[70] Q. Sun, A. Patney, L.-Y. Wei, O. Shapira, J. Lu, P. Asente, S. Zhu, M. Mcguire, D. Luebke, and A. Kaufman. Towards virtual reality infinite walking: Dynamic saccadic redirection. *ACM Trans. Graph.*, 37(4), jul 2018.

[71] K. Vasylevska, B. I. Kovács, and H. Kaufmann. Vr bridges: Simulating smooth uneven surfaces in vr. In *2020 IEEE Conference on Virtual Reality and 3D User Interfaces (VR)*, pp. 388–397, 2020.

[72] T. Wada, H. Konno, S. Fujisawa, and S. Doi. Can passengers' active head tilt decrease the severity of carsickness?: Effect of head tilt on severity of motion sickness in a lateral acceleration environment. *Human Factors*, 54(2):226–234, 2012.

[73] W. H. Warren and D. J. Hannon. Direction of self-motion is perceived from optical flow. *Nature*, 336(6195):162–163, 11 1988.

[74] D. M. Whittinghill, B. Ziegler, T. Case, and B. Moore. Nasum virtualis: A simple technique for reducing simulator sickness. In *Games Developers Conference (GDC)*, p. 74, 2015.

[75] C. Widdowson, I. Becerra, C. Merrill, R. F. Wang, and S. LaValle. Assessing postural instability and cybersickness through linear and angular displacement. *Human Factors*, 63(2):296–311, 2021.

[76] B. Wu, T. L. Ooi, and Z. J. He. Perceiving distance accurately by a directional process of integrating ground information. *Nature*, 428(6978):73–77, 3 2004.

[77] F. Wu, G. S. Bailey, T. Stoffregen, and E. Suma Rosenberg. Don't block the ground: Reducing discomfort in virtual reality with an asymmetric field-of-view restrictor. In *Symposium on Spatial User Interaction*, pp. 1–10. ACM, New York, NY, USA, 11 2021.

[78] F. Wu and E. S. Rosenberg. Combining dynamic field of view modification with physical obstacle avoidance. In *2019 IEEE Conference on Virtual Reality and 3D User Interfaces (VR)*, pp. 1882–1883. IEEE, 3 2019.

[79] F. Wu and E. S. Rosenberg. Asymmetric lateral field-of-view restriction to mitigate cybersickness during virtual turns. In *2022 IEEE Conference on Virtual Reality and 3D User Interfaces (VR)*, pp. 103–111. IEEE, 3 2022.

[80] F. Wu and E. Suma Rosenberg. Adaptive field-of-view restriction: Limiting optical flow to mitigate cybersickness in virtual reality. In *Proceedings of the 28th ACM Symposium on Virtual Reality Software and Technology*, VRST '22. ACM, New York, NY, USA, 2022.

[81] T. Yamamoto, J. Shimatani, I. Ohashi, K. Matsumoto, T. Narumi, T. Tanikawa, and M. Hirose. Mobius walker: Pitch and roll redirected walking. In *2018 IEEE Conference on Virtual Reality and 3D User Interfaces (VR)*, pp. 783–784. IEEE, 3 2018.

[82] G. Zhao, J. Orlosky, S. Feiner, P. Ratsamee, and Y. Uranishi. Mitigation of vr sickness during locomotion with a motion-based dynamic vision modulator. *IEEE Transactions on Visualization and Computer Graphics*, 2022.

[83] D. Zielasko, B. Weyers, and T. W. Kuhlen. A non-stationary office desk substitution for desk-based and hmd-projected virtual reality. In *2019 IEEE Conference on Virtual Reality and 3D User Interfaces (VR)*, number March, pp. 1884–1889. IEEE, 3 2019.